Int. J. Electrochem. Sci., 10 **(2015)** 10806 - 10820

International Journal of
ELECTROCHEMICAL
SCIENCE
www.electrochemsci.org

Study of Grain Boundary Characters under Intergranular Corrosion in Copper Conductor and Its Relationship with Paper Oil Insulation in Transformer

Yuan Yuan[1,*], *Xiao He*[2], *Zhilong Xu*[1], *XinLiang Guo*[2], *HuanHuan Xia*[2]

[1] College of Materials Science and Engineering, Chongqing University, Chongqing, China 400044
[2] Electric Power Research Institute of Yunnan Power Grid Co., Ltd.
[*]E-mail: yuany@cqu.edu.cn

Received: 2 March 2015 / *Accepted:* 4 October 2015 / *Published:* 4 November 2015

The properties of materials such as corrosion, creep resistance, and weld ability are relevant to special and random grain boundaries which belongs to the category of Grain Boundary Engineering (GBE). Recently, failures of transformers and reactors due to corrosive sulfur compounds in transformer oil is reported in literatures. This article takes paper oil insulation system as the research object, using Electron Backscatter Diffraction (EBSD) study the grain boundaries of copper conductor in insulating oil containing dibenzyl disulfide (DBDS), and the features corrosion pits. For paper insulation, the breakdown voltage and the microstructure of paper were presented. The paper insulation produced plenty of substances, such as metallic particles and fiber, water, dissolved gas, furfuraldehyde, dissolving in oil during the thermal aging. To gain further insight into the involvement of dielectric properties of insulation oils, ion mobility was tested through the approach by reversal polarity.

Keywords: Grain boundary engineering; copper; corrosion pits; dibenzyl disulfide; breakdown voltage; ion mobility

1. INTRODUCTION

Corrosive sulfur in mineral insulating oils in transformer is one of the serious issues affecting the lifetime of the transformers. Several studies have indicated that active sulphur should be responsible for this problem. Crude oil contains hundreds of sulphur compounds of which acts as antioxidants beneficial to oil while others are side-effect towards metals in transformers. Available datas over the past several years have confirmed that dibenzyl disulfide (DBDS) is overriding substance leading to the sedimentation of copper sulfide on insulating paper[1].

Great efforts and different points of view were being made to explain and relieve corrosion problems due to active sulphur in transformer. Lewin and Jarman put forward that when the local temperature was maintained at a high level for short time, sulphide will deposits on copper surface due to the gassing of hydrocarbon compounds possessing sulphur and/or H_2S gas from sulphurous mineral insulating oil[2]. Toyama, Mizuno[3] think that both Cu-DBDS and Cu-DBPC complex are able to transfer from copper conductor into Kraft paper and then copper sulfide will break down on Kraft paper. Hajek[4] described that copper sulfide are the result of the reaction of copper conductor with mercaptan.

As been reported, same points can be summarized that they all focused on insulating paper and oil. However, corrosion mechanism of copper in transformer oil containing dibenzyl disulfide was not be focused on. Ralston[5] revealed that grain boundaries were correlated with corrosion rate of metals. It is well known that grain boundary types have a significant influence on the intergranular corrosion behavior of a polycrystalline materials [6]. "Special boundary" could be defined that has better corrosion properties compared to a random boundary. These special boundaries are known as coincident site lattice boundaries (CSLs). CSL boundaries are denominated by the symbol Σn (1/n is the fraction of lattice points belonging to the coincident lattice)[7]. Generally speaking, boundaries with $\Sigma \leqslant 27$ were regarded as special while boundaries with $\Sigma > 27$ were considered random[8]. Not only the fraction of special boundaries are desired to increase, but also the network of triple junctions that these boundaries are a part of it should be considered[9].

The purpose of this study was to examine the effects of grain boundary characters of copper conductor in transformer oil containing dibenzyl disulfide and the relation was discussed between "grain boundary engineering" (GBE) and corrosion behavior under the condition of thermal aging. This study elucidated the functional role of grain boundary character and triple junctions of copper against corrosion which may provide novel idea for improving the corrosion resistance of copper wires. Meanwhile, author will contact oil -paper with copper windings in accelerated thermal aging process.

2. EXPERIMENTAL

2.1 Preparation of Samples

The experimental condition was presented in Table 1. Oil and copper conductor wrapped with insulation paper were placed together in a 350 ml vial. The vials were heated in the furnace to sustain a homoiothermy with a temperature deviation of 1°C in vacuum environment, vacuum degree is 133 pa. Specimens were heated for 15 days at 150°C. The paper-wrapped copper windings provided by Chongqing ABB Transformer Co., Ltd and the windings were immersed in the tested oils. Chemical composition of copper in transformer was showed in Table 2.

Table 1. Condition of experimental

Copper conductor	**60mm×8.5mm×3.5 mm**
Paper	wrapped with a two layers of insulating paper
Oil	350ml
Heating time	15days
Temperature	150℃
DBDS	0, 200,500,1000ppm
Vacuum	≤133pa

Table 2. Chemical Composition of T2 copper in transformer (in wt. %)

Cu + Ag	Zn	Ni	Sb	Bi	Pb	Fe	S	As	O	Sn
≥99.90	**≤0.005**	**≤0.005**	**≤0.002**	**≤0.001**	**≤0.005**	**≤0.005**	**≤0.005**	**≤0.002**	**≤0.06**	**≤0.002**

2.2. Characterization of copper conductors.

Electron backscattered diffraction (EBSD) was applied to measure grain boundary crystallographic parameters using the orientation imaging microscopy (OIM) system installed on a *Zeiss AURIGA FIB* was used for collecting and indexing diffraction patterns. The representative spatial resolution obtained with the EBSD technique is about 1 μm.

2.3 Performance parameter analysis methods of insulating paper

Breakdown voltage studies were carried out with a power frequency high voltage breakdown test platform which contains transformer and electrodes. In this test, we selected mineral oil as medium (25# Karamay oils), and the diameter of the electrode was 1.5 cm, each sample tested fifteen times, obtain Weibull distribution of power frequency breakdown data[12]. Weibull parameters of power frequency breakdown data of insulating papers were showed in Table 3. X-ray diffraction measurements were carried out on a *Empyrean XRD* system using Cu Ka radiation(40kV,40mA and k=0.154nm) over a range from 5° to 60°at a scan speed of 2°/min.

Table 3. Weibull parameters of power frequency breakdown data

The aging time of sample/day	**Weibull parameters**	
	Scale parameter	Shape parameter
0	11.21	20.18
5	11.75	30.88
10	11.54	25.17
15	12.11	16.48

2.4 Characterization methods of insulating oil

Isothermal transient ionic current acquired by utilizing voltage polarity reversal [11] was applied in this paper to obtain ions mobilities in insulating oil specimens. In the process of experiment, a step voltage was applied to the test cell to shift the ions from the oil bulk and to gather them in electrode surfaces. Then, voltage polarity was suddenly inversed (the conversion time of the voltage shift was much shorter than the transit time of ions). By reversing the voltage polarity, the ions aggregated at the electrodes surfaces were forced to migrate towards the opposite electrodes and the time to peak (TTP) in the recorded current traces could gain their average mobility. Through this process, the ions mobility μ can be calculated as[12, 13].

$$\mu = \frac{d^2}{U.TTP} \quad (1)$$

Where U is the applied voltage, d is the gap length, equal to 2mm. It is hypothesis that the time to peak was approximately equal to the transit time needed for ions to cross the oil gap between electrodes.

3. RESULTS AND DISCUSSION

3.1 The corrosion mechanism of copper windings in the insulating oil

Figure.1a shows the EBSD map of the microcrystalline copper sample when the concentration of DBDS is 500ppm. The average grain size is 5.1565μm, the image quality (IQ) map in Figure.1b shows the different types of boundaries. Black arrows show random high angle boundaries and gray lines indicate all coincident site lattice boundaries (CSLs). In Figure.1b, Some of grains are coherent twins on account of they are characterized by their parallel-sided arrangement[14]which marked as red arrows.

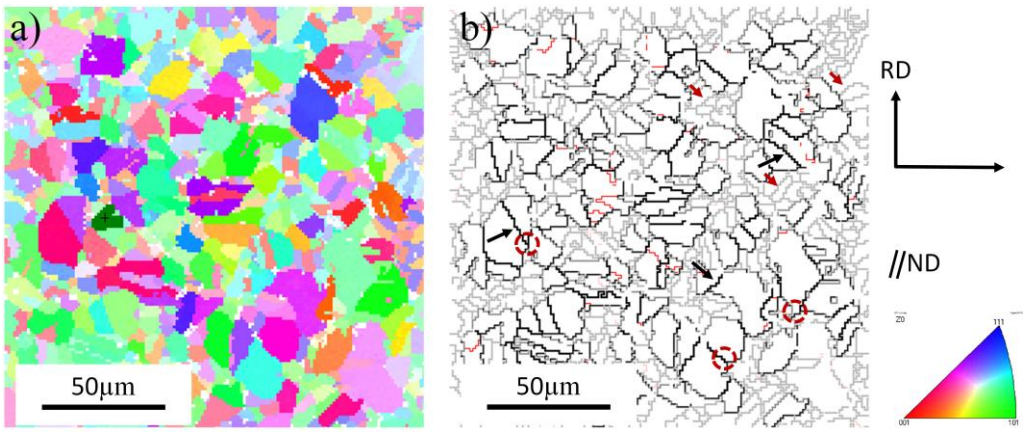

Figure 1. Part of an EBSD map of copper conductor in which a fine grain size was 5.1565μm: The random boundaries were shown in bold dark lines while the special boundaries were indicated in the lighter gray scale as thin lines. Indicated by the red arrows in the grain boundaries were twin boundaries. Triple junctions were marked as the red circle.

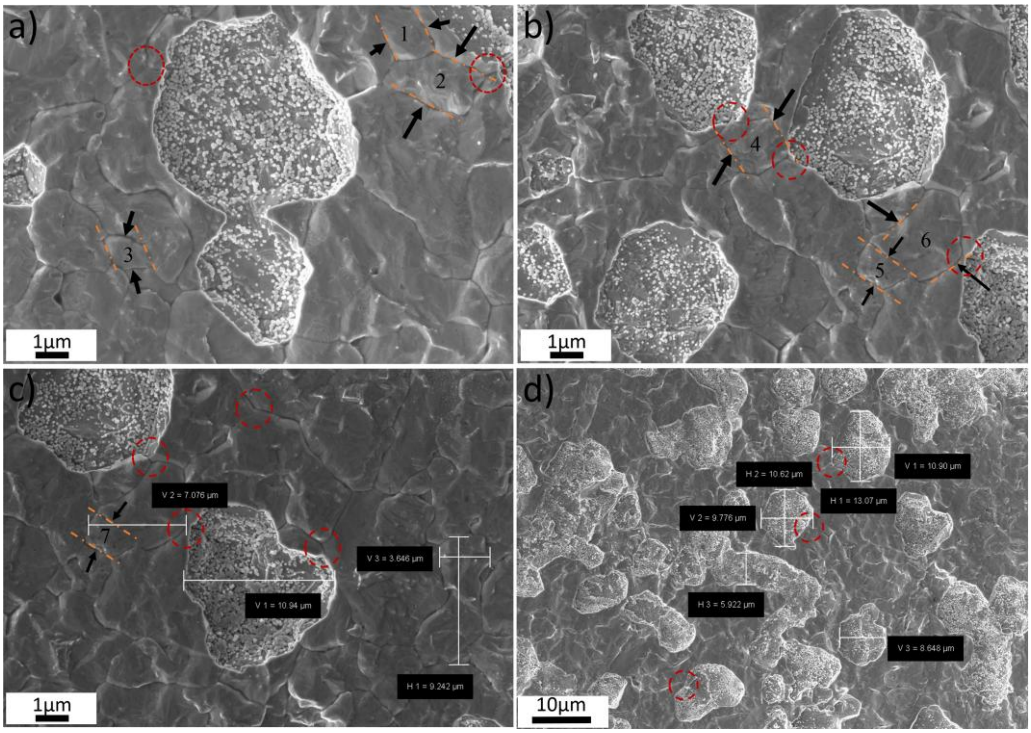

Figure 2. SEM images of copper corrosion. (a) The grains labeled as 1, 2, 3, they are coherent twins since they are characterized by their parallel-sided arrangement (marked as yellow parallel lines); (b, c) grains labeled as 4, 5, 6, 7 were coherent twins. All corrosion pits have a shape of curve, and all straight boundaries were found have good corrosion resistance properties in pictures.

Triple junctions are marked as the red circles. Literature confirmed that the low grain boundary energy of the coherent twin boundaries on copper, and have good corrosion resistance properties [15]. In order to confirm this theory, SEM was used to observe the surfaces of copper after corrosion when the concentration of DBDS is 500ppm. SEM micrographs Figure 2 (a) – (d) showing corroded surfaces after thermal aging tests. This section the author focuses on two aspects: (1) Σ3s of coherent twin boundary have good corrosion resistance properties. (2) The distribution characteristics of triple junctions in network of grain boundaries.

Intergranular corrosion were observed, corrosion tendency was presented in Figure 3. SEM micrographs revealed that the bigger the grain, corrosion occurs preferential in the process of corroding. Among all grain boundaries, all corrosion pits have a shape of curve, and all straight boundaries were found have good corrosion resistance properties, It can be then concluded that a straight grain boundary has a very high probability to be a ‘coherent twin boundary’ and that a curved grain boundary can be cataloged either as random high angle boundary or non-coherent 3 boundary[16]. A considerable attack was observed for the curved grain boundary. The magnitude of intergranular corrosion is determined by both the grain size and the shape of grain boundary. As already mentioned, the straight grain boundary is assigned to the category of coincident site lattice boundaries (CSLs) which include coherent twin grain boundaries

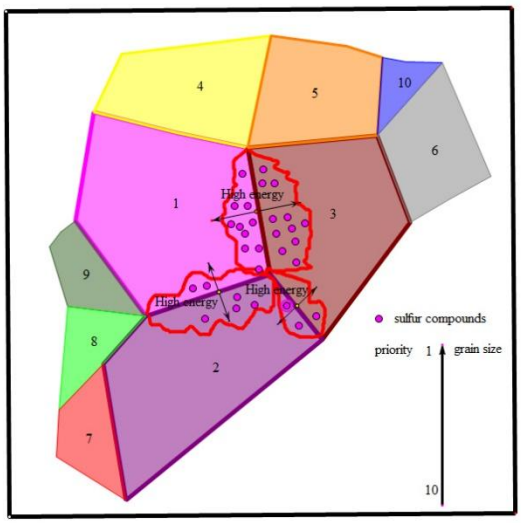

Figure 3. Corrosion tendency of copper conductor.

From the perspective on the morphology of corrosion pits, all corrosion pits have a shape of curve due to random boundary present the curve shape and closely relevant to their energies: the higher the boundary energy, the greater corrosion degradation of the surface region[17]. In figure 2(a), the grains labeled as 1, 2, 3, they are coherent twins due to they are characterized by their parallel-sided arrangement[14]. In figure 2(b) (c), grains labeled as 4, 5, 6, 7 were coherent twins. Due to the existence of these grains, hindered the combination between corrosion pits preventing the corrosion effectively. In figure (d), due to the lack of the existence of the special grain boundary, a considerable proportion of corrosion pits mutual contacting which expand corrosion degree. Generally speaking, a special boundary can be defined as one that has better properties than an average boundaries, and often CSLs are classified as special boundaries. However, this is a misdirect classification because in general, apart from Σ3, the properties of CSLs are similar to random boundaries in three-dimensional polycrystals[7]. Moreover, Σ3s not always show good properties unless coherent twins on {111} planes. However, mounting evidence suggests that CSLs should be a misorientation-based classification and particular interface plane does not exist. Meanwhile, the geometry of a grain boundary should be described by five ‘degrees of freedom’ which can be decomposed into to three degrees of freedom distributed to the misorientation and two to the grain boundary plane instead of oversimplifying grain boundary geometry[18]. Generally, all Σ3s possess potential properties that are different from random boundaries while the real property distribution depend on the boundary planes of which the Σ3s is constituted to a large extent. Therefore, we should take both grain boundary plane and misorientation into consideration.

Recently, a developmental milestone advance have been developed to evaluate statistically the distribution of plane types. One of the planes at a boundary which belongs to systems favour asymmetric boundaries possessing a low index, namely, low energy-plane[19]. In fact, researchers have recently demonstrated that general grain boundary population have a preference for misorientations on <110> and <111> exist frequently which both can bring in {111} planes. Additionally, <110> misorientations are geometrically essential on account of multiple twinning

interactions generate a higher than random proportion of Σ9, Σ27a and Σ27b[20]. If one side of the boundary has a low index plane, the plane indices of the boundary for the other side are defined by the misorientation. Tilt boundaries have a zero twist angle with particularly low energies, such as the coherent annealing twin on {111}[7],which can be regarded as transparent example. Hence, we can break up the boundary network by boundaries misoriented on <110> and <111>, especially twins, to regulate special boundary. In this way, we can increase the percentage of boundaries possessing at least one low index plane, usually {111}. To improve the properties of copper conductor obviously, we can adjust and control index plane in general random boundaries as well as in Σ3s.

The triple junctions were characterized after *Fortier et al*[21, 22] and classify as follows : type one is three special boundaries (3S or 3-CSL), type two is two special boundaries and one random boundary(2S-R or 2-CSL), type three is one special and two random boundaries (S-2R or 1-CSL), type four is three random boundaries (3R or 0-CSL) [9]. The network connection of special boundaries will be increased if add in 2-CSL and 3-CSL junctions at the cost of 0-CSL and1-CSL while the connectivity of random boundaries will accompanied decrease. By eliminating short section from the network decompose a large network of random grain boundaries into small clusters.

Within a grain, annealing twins which formed during grain boundary engineering often come into being parallel coherent Σ3 boundaries[23]. The abundant annealing twinning related to GBE induce ‘‘multiple twinning”, while a Σ9 boundary produced by two Σ3 boundaries meet at a triple junction and can be described as $\Sigma3+\Sigma3 \rightarrow \Sigma9$[24]. Higher order $\Sigma3^n$ boundaries are developed alike, e.g., $\Sigma3 + \Sigma9 \rightarrow \Sigma27$. Reversely, higher order $\Sigma3^n$ boundaries can convert to low order, e.g., $\Sigma3 + \Sigma9 \rightarrow \Sigma3$. This mechanism is generalized express as the ‘‘Σ3 regeneration mechanism” which presents that $\Sigma3^n + \Sigma3^{n+1} \rightarrow \Sigma3$ occur more frequently at triple junctions than $\Sigma3^n + \Sigma3^{n+1} \rightarrow \Sigma3^{n+2}$[25].

In figure 2, due to parallel coherent Σ3 boundaries of twin grains (marked as yellow parallel lines), preventing the fusion of two corrosion pits effectively, set corrosion back. Multiple twinning can break the random network into many separated places so that diminish the random cluster size that could enhance corrosion resistant properties of copper conductor. In materials of GBE, annealing twins (surround by coherent Σ3 boundaries) lead to the increase in special fraction directly, and also indirectly when twin boundaries contact with random boundaries to produce low-Σ boundaries[26, 27].

Grain size is determinant factor that affect the issues of connectivity and distribution in grain boundary networks. In this paper, author pay attention to analyze two-dimensional clusters for which the grain size substituted by the mean linear intercept[28]. The quantitative study to abide by dimensionless units of length, where measured length is standardized by $\bar{L}$, to boost comparison between microstructures[23]. Independent grain boundary network was confirmed by their shape and size introducing standard measures from percolation theory[29]. A cluster marked as S, namely, the mass fraction of grain boundary networks which defined as the whole (dimensionless) length of boundaries contained in cluster. Generally, a cluster was constitutive of N discontinuous units (i.e., boundaries or boundary segments), the radius of gyration Rg of a cluster is defined as:

$$Rg^2 = \frac{1}{N}\sum_{i=1}^{N}\left|\boldsymbol{r}_i - \boldsymbol{r}_o\right|^2 \qquad (2)$$

While r_o is defined as the mean distance of a boundary from its center of mass

$$\boldsymbol{r}_o = \frac{1}{N}\sum_{i=1}^{N}\boldsymbol{r}_i \qquad (3)$$

Among formula, r_i was a vector directing to the position of the ith boundaries or boundary segments

From above, the properties of individual clusters was described. However, mean measures of the total clusters population maybe more typical of the microstructures. The weighted average cluster mass is presented by:

$$< S >= \frac{\sum_S s^2.n_s}{\sum_S s^2.n_s} \qquad (4)$$

Where n_s is defined as a distribution function of cluster mass, which express the number of clusters of size s per unit area[29].Meanwhile, a weighted average diameter of gyration can be expressed by *correlation length* effectively:

$$\xi^2 = \frac{2\sum_S R_g^{\,2} s^2.n_s}{\sum_S s^2.n_s} \qquad (5)$$

The largest linear dimension of any interconnected grain boundary networks, D_{max}, is identified by the above equation.

For properties, e.g., intergranular corrosion controlled merely by continuous weak-link paths along grain boundaries, or we assumed that random boundaries are property-controlling in some situations, then maximum length, D_{max}, can be applied to predict the performance of materials in microstructure[30-33]. In this work, we have not measured this parameter in copper conductor, a correlation of D_{max} with property measurements of copper will be the subject of future work ,and it could serve as an important standard for evaluate quality grade of transformer conductor.

Results presented in this section have shown that break up the connectivity of the random grain boundary network is effectively accomplished by the integration of Σ3 twin boundaries into the network of boundaries. The Σ3 twin boundaries showed an increased resistance to intergranular corrosion compared to random grain boundaries.

3.2 The performance of the paper insulating after thermal aging

The scanning electron microscope (SEM) is capable of displaying high-resolution images of a specimen surface. The degree of degradation of insulating paper were performed in Figure 4. Figure 4 (a) presented smooth cellulose fibers with no signs of thermal deformation before aging, the mean width of the cellulose fibers was about 30μm. However, some obvious changes have taken place as time goes by. Figure 4 (b) is a SEM image of the insulating paper with 1.35K X magnification after 15 days of thermal aging with DBDS of 1000ppm. The average width of the cellulose fibers turn smaller, displacement and deformity appeared in the cellulose fiber's wall. Holes appeared on the celluloses on account of copper sulfide deposited on insulating paper and easy to accumulate in together which made

insulating paper thermal conductivity performance degradation leading to local overheating. However, when local overheating occurs, copper sulfide deposition would generate in the limited areas abundantly [34]. Therefore, insulating paper will fall into "Local overheating $\overset{More}{\Longleftrightarrow}$ Copper-sulfide" vicious cycle.

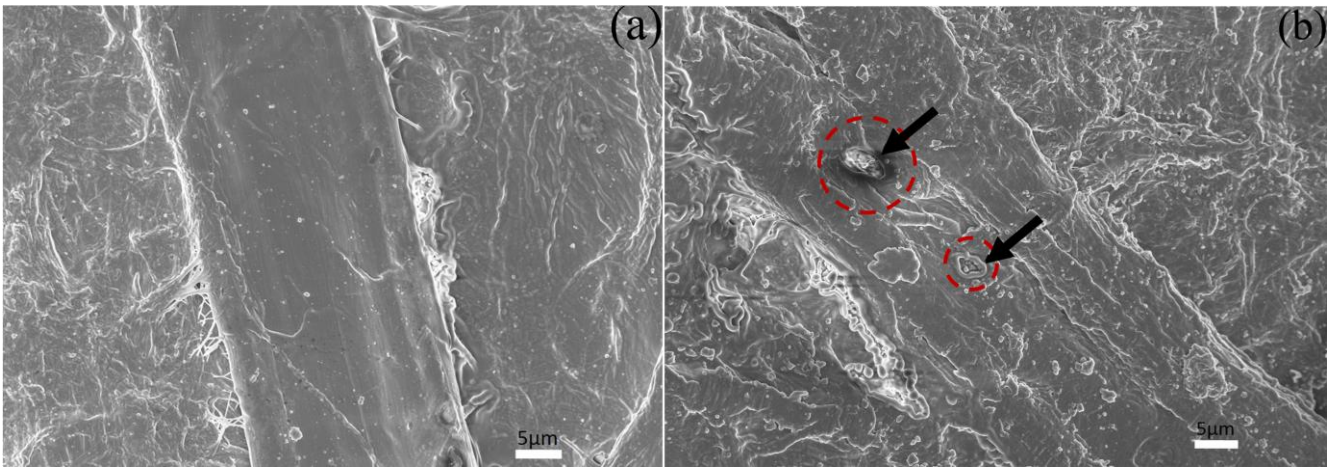

Figure 4. SEM images of degree of degradation of the transformer insulating paper. (a) un-aged paper (b) After 15days of thermal aging with 1000ppm concentration of DBDS at 150℃. Black arrows indicated holes on cellulose.

The crystallinity and crystal structure largely decided electrical performance of crystalline polymer materials. Crystal structure identification and chemical phase analysis can be performed by analyzing the length, width, height and diffraction angle. So, it is extremely useful in the investigation of the crystal structures of the cellulose fibers in insulating paper by XRD analysis[35]. The XRD spectrums of tested transformer insulating paper specimens showed in Figure 5, there is some smooth diffraction peaks and a sharp diffraction peak, both amorphous regions and crystalline regions can be obtained from diffraction peaks. In insulating paper, crystalline regions mean compact and well-organized. Conversely, the amorphous regions turn out to be irregular, disordered and deteriorate more easily. The relative crystallinity of the insulating paper can be calculated using following equation[36]:

.

$$CrI = \left[\left(I_{002} - I_{am} \right) / I_{002} \right] \times 100\% \quad (6)$$

Where: *CrI* is relative crystallinity. I_{002} is diffraction intensity of crystalline regions. I_{am} is diffraction intensity of amorphous regions.

Diffraction peaks of insulating paper have some shifting which may be the consequence of resetting the crystal lattice with thermal aging process. However, with different process of thermal aging time, the position of intensity peak in the 2theta spectrum remains unchanged. Results means that the crystal type of insulating paper has not changed radically. The intensity and relative crystallinity of insulating paper was presented in Table 4. It indicated that the relative crystallinity (*CrI*) of insulating paper decreased from 73.44% to 68.12% in the earlier stage of 5 days and turned to flat with tiny fluctuation from 5 days to 15 days in aging process. During thermal aging process, the

relative density and the width of cellulose fibers showed in SEM diminish in line with the decrease of relative crystallinity.

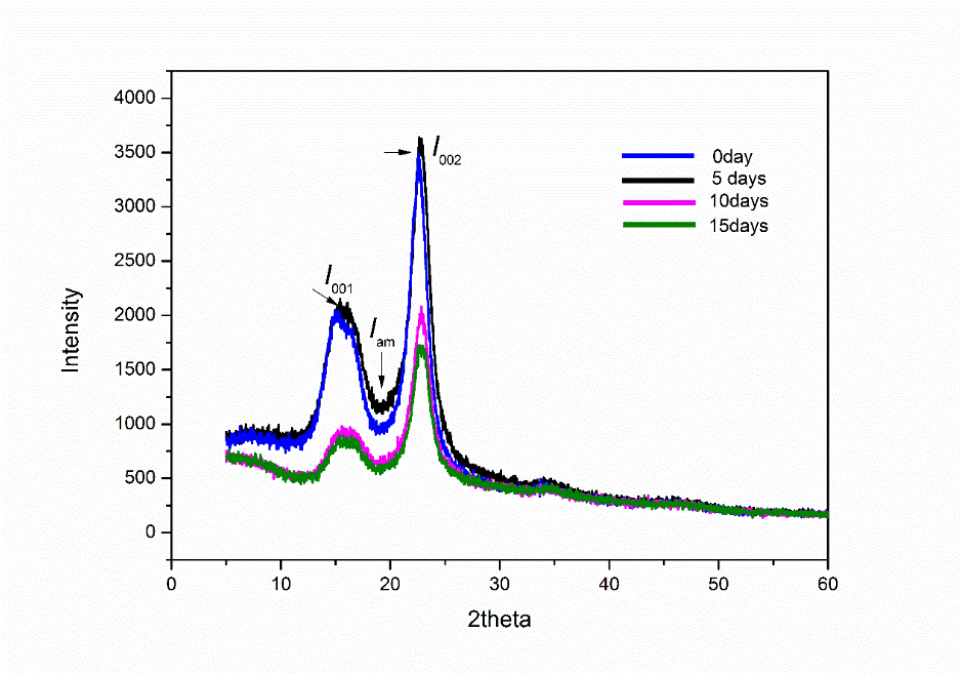

Figure 5. XRD spectrum of tested insulating paper.

Table 4. The intensity and relative crystallinity of insulation paper

Transformer insulation paper	Intensity		Relative Crystallinity / *CrI*
	I_{002}	I_{am}	
Un-aged	3434	912	73.44%
Aging for 5days	3567	1137	68.12%
Aging for 10days	2007	660	67.12%
Aging for 15days	1716	566	67.02%

Weibull distribution of power frequency breakdown data was showed in Figure 6. Overall, the breakdown voltage of insulating paper have a tiny decline after thermal aging, breakdown voltage drop up from 13.49kv-11.75kv to 10.72kv-11.75kv. Corrosive sulfur compounds as a conductor material, deposited in the surface of the insulating paper, reducing the breakdown voltage of insulating paper. According to combining the theory of dielectric ageing trap, under the effect of high electric field, electronic inject into conduction band of dielectric material by Schottky or Fowler Nordheim effect from cathode. Once injected, electron quickly fall into the trap after several electron scattering with the reason that electron mean free path is short, and possess high local density of states. In the process of electronics into the trap and de-trap, electronic from high-energy state to low-energy state, excess energy transferred in the form of radiating to another electron which turn to the hot electrons [37], increasing the cellulose chain damage of medium internal, reduce the physical and chemical properties, shorten its insulation life.

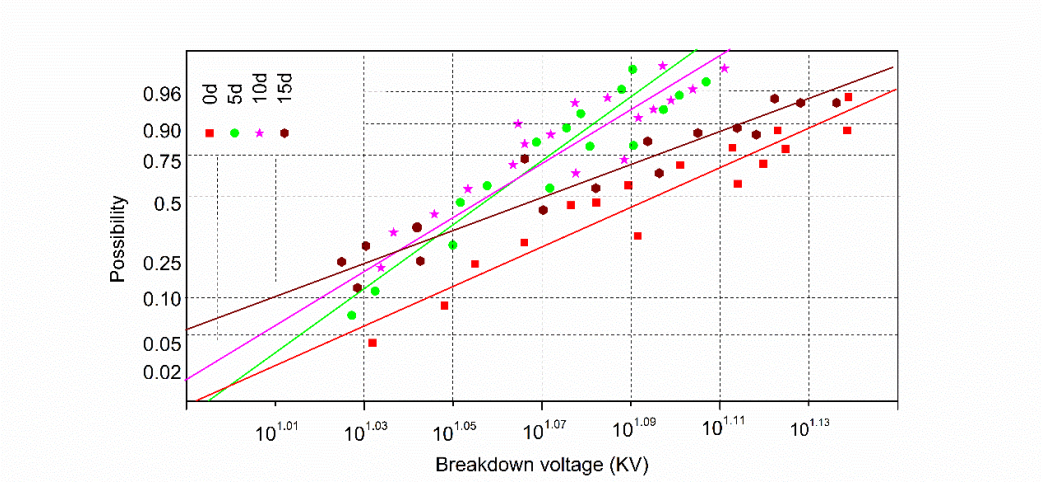

Figure 6. Weibull distribution of power frequency breakdown data

The microstructures topography and breakdown data studies indicated that the surface roughness of insulation paper after thermal aging increased clearly, charged particles in the surface of paper increased, and the ability of charge collection of paper enhanced. Insulating paper will fall into "Local overheating$\overset{More}{\Longleftrightarrow}$ Copper-sulfide" vicious cycle under the accelerated thermal aging.

3.3 Mobility of ions in the transformer oil

Mobility of ions is an inherent characteristic of a particular type of charge carriers migrating in a specific condition and, therefore, can be differentiated as a unique characteristic parameter of each dielectric liquid[38].In this experiments, a controllable thermal chamber containing test cell was applied to perform the measurements. Keithley 6517A electrometer was utilized as both ampere meter and the voltage source. In order to measure the true mobility, a low voltage should be applied to avoid electrohydrodynamic (EHD) [39], So the experiment voltage selected 40kv. Representative curves of the current of positive ions reported for the four specimens were shown in Figure 8. The current in oil A which contains 1000ppm DBDS has the largest value of the amplitude and utilizes the shortest time to current peak. The higher the DBDS concentration, the smaller the TTP which can be correlated with chemical constituents, such as metallic particles and fiber, water, dissolved gas, furfuraldehyde, dissolving in oil during the thermal aging. The ions mobility of dielectric fluids are inversely proportional to viscosity of the fluids, η, on the basis of Walden's rule [40],equation can be expressed as:

$$u\eta = const \quad (7)$$

Meanwhile, according to Stokes' rule, the relationship between the effective ionic radius, R, and ion mobility

$$U = \frac{e}{6\pi\eta R} \quad (8)$$

One can obtains (9) by combining equations (7) and (8)

$$u\eta = e / 6\pi\eta R = Const \quad (9)$$

The values of R could be acquired from above. Adamczewski [41] have demonstrated that mobility of ions of multifarious hydrocarbon liquids were suitable for equation (8) so that effective radii of the ionic carriers could be figured out through this method. Through calculate the effective radius of ions, the distance between ions in oil within which they interact effectively with each other can be obtained. The results of the calculations of the ionic radii for this research are presented in Table 5 .Under the condition of 40 degrees, the vaule of 25# kinematic viscosity was provided by the manufacturers. Further, the values of η were obtained as the products of the measured magnitudes of the kinematic viscosity and typical oil densities at 40 degrees. From Table 5, effective ionic radius turn smaller with the increase of DBDS concentration. This could be explained with the effects of acids, metallic particles, water and other impurities on the mobility which produced as the aging process. Ions mobility in insulation oil has an effect on the dynamics of an electric field distribution in oil gaps in transformer. Measurement of positive and negative ion mobility helps to improve accuracy in the evaluation of insulating oil aging condition and define apparent properties of the insulating oil and acted as a "bridge" between copper-paper-oil systems.

Figure 7. Keithley 6517A electrometer with controllable thermal chamber

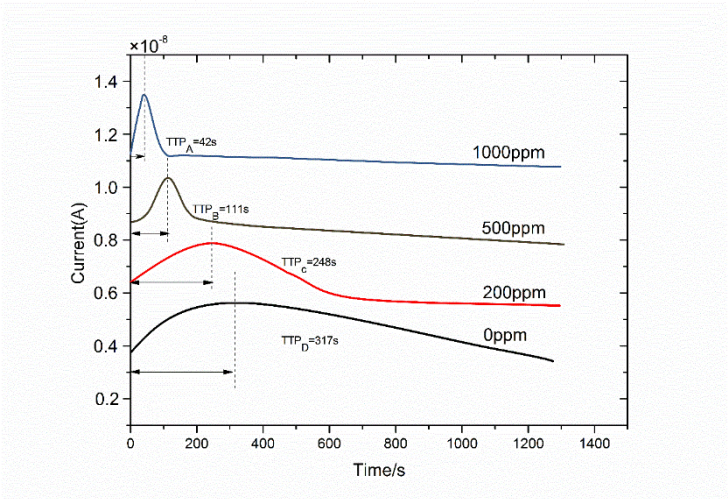

Figure 8. Typical traces of the current of positive ions recorded for the four samples after polarity reversal

Table 5. Measurement of ion mobility in dielectric Liquids (μ) and effective ionic radii for investigated oils (R)

Samples	Kinematic viscosity (10^{-6} m^2/s)	Density (kg/m^3)	η(10^{-3} Pa s)	μ (10^{-9} m^2/Vs)	R (10^{-9} m)
0ppm	8.6	867	8.2	0.32	3.2
200ppm	7.8	844	7.7	0.40	2.8
500ppm	7.5	837	6.9	0.90	1.3
1000ppm	6.4	828	6.4	2.38	0.56

3.4 The connection about the oil - paper - copper systems

Copper sulfide formation mechanism and its connection with the oil - paper - copper in DBDS containing oil was discussed. From the viewpoint of copper conductor, the corrosion process can be divided into three stages. At stage 1, corrosion starts from grain boundary, along the grain boundary etching the whole grain slowly, which form corrosion pits. At stage 1, corrosion pits were small and independent of each other, copper compounds in corrosion pits was less. When a whole grain was etched, there are two corrosion trend in stage 2, one is that the area of the corrosion pit grow and begin fusion with surrounding pits. Not only the area of the corrosion pit grow, but also turn deep. At stage 3, corrosion pits connected with each other, copper compounds achieve the maximum. However, Σ3 twin boundaries break up the connectivity of the random grain boundary network, enhancing corrosion resistant properties of copper conductor. Copper sulfide on insulating paper was observed with the help of SEM, copper sulfide on insulating paper was deposited by the migration of copper complex from copper to insulating paper [3]. This would resulted in a decline in the breakdown voltage of the insulating paper and enhanced the probability of local overheating on paper surfaces. A variety of factors affecting on the aging of oil-paper insulation. The oil-paper insulation produced plenty of substance, such as metallic particles and fiber, water, dissolved gas, furfuraldehyde, dissolving in oil during the thermal aging[42]. All of this could be concluded as polarity ions, in this work, by measuring the ionic mobility and calculate the effective ionic radius, we could characterized the aging condition of insulating oil effectively and comprehensively.

4. CONCLUSIONS

Corrosion damages of copper conductor was macroscopically rather uniform whereas an obviously preferential grain boundary degradation and selective corrosion of some grains. The Σ3 twin boundaries presented an increased resistance to intergranular corrosion compared to random grain boundaries. Multiple twinning can interrupt the random network in many separated places, and thereby reduce the random cluster sizes that could enhance corrosion resistant properties of copper conductor. The corrosion process produced copper compounds, diffusing into oil and insulation paper. The microstructures topography and breakdown data studies indicated that the surface roughness of insulation paper after thermal aging increased clearly, charged particles in the surface of paper

increased, and the ability of charge collection of paper enhanced. Insulating paper will fall into "Local overheating$\overset{More}{\Longleftrightarrow}$ Copper-sulfide" vicious cycle under the accelerated thermal aging.

For transformer oil, the higher the DBDS concentration, the shorter the TTP, effective ionic radius turn smaller with the increase of DBDS concentration .Measurement of positive and negative ion mobility helped to improve accuracy in the evaluation of insulating oil aging condition and define apparent properties of the insulating oil, and acted as a "bridge" between copper-paper-oil systems, and characterized the aging condition of insulating oil effectively and comprehensively.

ACKNOWLEDGEMENTS
The authors gratefully acknowledge support provided by National Natural Science Foundation of China (51407018) and (51277187).

References

1. F. Scatiggio, V. Tumiatti, R. Maina, *IEEE T Power Deliver*, 23 (2008) 508.
2. P. Mitchinson, P. Lewin, P. Jarman, conference Record of the 2010 IEEE International Symposium, San Diego, June 6,2010,pp. 1-4.
3. S. Toyama, K. Mizuno, F. Kato, *IEEE T Dielect El In*, 18 (2011) 1877.
4. J. Hajek, M. Dahlund, L. Pettersson, *ABB review*, 3 (2004) 61.
5. K. Ralston, N. Birbilis, C. Davies, *Scripta Mater*, 63 (2010) 1201.
6. S. Kim, U. Erb, K. Aust, G. Palumbo, *Scripta Mater*, 44 (2001) 835.
7. V. Randle, *Scripta Mater*, 54 (2006) 1011.
8. T. Watanabe, *J. Phys. Colloques*, 46 (1985) C4-555.
9. M. Kumar, W.E. King, A.J. Schwartz, *Acta Mater*, 48 (2000) 2081.
10. S .Greek, F .Ericson, S .Johansson, *Thin Solid Films*, 292 (1997) 247
11. J. Filippini, C. Marteau , *IEEE T Dielect El In*, 1 (1994) 1000.
12. B. Dikarev, G. Karasev, R. Romanets, Proceedings of the IEEE 13th International Conference on. IEEE, Nara, Jul 20 - Jul 25, 1999,pp. 33-36.
13. M. Watanabe, K. Sanui, N. Ogata, *J. Appl. Phys*, 57 (1985) 123.
14. M. Kumar, A.J. Schwartz, W.E. King, *Acta Mater*, 50 (2002) 2599..
15. L. Lapeire, E. Martinez Lombardia, K. Verbeken, *Mater. Sci. Forum*,783 (2014) 1658.
16. E. Martinez-Lombardia, L. Lapeire, V. Maurice, *Electrochem Commun*, 41 (2014) 1.
17. M. Yamashita, T. Mimaki, S. Hashimoto, S. Miura, *Philos. Mag. A*, 63 (1991) 707.
18. D. Wolf, S. Yip, Materials interfaces: atomic-level structure and properties, *Springe*r, 1992.
19. G.S .Rohrer, D.M .Saylor, B.E. Dasher,Wynblatt P. Z *Metall*, 95 (2004) 197.
20. V.Y. Gertsman, C. Henager Jr, *Interf Sci*,11 (2003) 403.
21. P. Fortier, K. Aust, W. Miller, *Acta Metall. Mater*, 43 (1995) 339.
22. P. Fortier, W. Miller, K. Aust, *Acta Mater*, 45 (1997) 3459.
23. C.A. Schuh, M. Kumar, W.E. King, *Acta Mater*, 51 (2003) 687.
24. V. Randle, G. Rohrer, H. Miller, M. Coleman, G. Owen, *Acta Mater*, 56 (2008) 2363.
25. V. Randle, *Acta Mater*, 47 (1999) 4187.
26. V. Gertsman, K. Tangri, Acta *Metall.Mater*, 43 (1995) 2317.
27. P. Lin, G. Palumbo, K. Aust, *Scripta Mater*, 36 (1997) 1145.
28. P. Villars, L.D. Calvert, Pearson's handbook of crystallographic data for intermetallic phases, American Society for Metals Metals Park, OH, 1985.
29. D. Stauffer, A. Aharony,.Introduction to percolation theory. Taylor and Francis ,London, 1992.

30. G. Palumbo, P. King, K. Aust, U. Erb, P. Lichtenberger, *Acta Metall Mater*, 25 (1991) 1775.
31. K. Aust, U. Erb, G. Palumbo, *Mater. Sci. Eng.* A, 176 (1994) 329.
32. V. Gertsman, M. Janecek, K. Tangri, *Acta Mater*, 44 (1996) 2869.
33. V. Gertsman, K. Tangri, *Acta Mater*, 45 (1997) 4107.
34. T. Amimoto, E. Nagao, J. Tanimura, S. Toyama, N. Yamada, *IEEE T Dielect El In*, 16 (2009) 257.
35. R.-j. Liao, C. Tang, L.-j. Yang, S. Grzybowski, *IEEE T Dielect El In*, 15 (2008) 1281.
36. L. Segal, J. Creely, A. Martin, C. Conrad, *Text. Res. J*, 29 (1959) 786.
37. Z. Yewen, Y. Baitun, T. Demin, L. Yaonan , Annual Report., Conference on IEEE. Leesburg, VA, Oct 29- Nov 2, 1989,pp.303-308.
38. L. Yang, S.M. Gubanski, Y.V. Serdyuk, J. Schiessling, IEEE T Dielect El In , 19 (2012) 1926.
39. P. Atten, *IEEE T Dielect El In*, 3 (1996) 1.
40. D. Andre, IEEE International Conference. Trondheim, June 26-30, 2011, 1-11.
41. I. Adamczewski, Taylor and Francis, London, 1969.
42. A. Emsley, G. Stevens, *IEE P-Sci Meas Tech*, 141 (1994) 324.